DOI:10.5937/IIZS26194H

ROUND-TRIP EFFICIENCY (RTE) OF HOME BATTERY STORAGE SYSTEMS UNDER TROPICAL CLIMATIC CONDITIONS - A CASE STUDY OF THAILAND

Research paper

Matthias Hauer[1]*, Ashish Srivastava[2], Momir Tabaković[3]
[1]FH Technikum Wien, Vienna, Austria

Abstract: Residential battery-storage efficiency is commonly reported under moderate reference conditions, whereas systems installed in tropical climates may experience substantially higher ambient temperatures. This paper investigates the DC-side round-trip efficiency (RTE) of a residential lithium iron phosphate ($LiFePO_4$) battery under representative Bangkok conditions using a reduced-order electro-thermal model. A constant 25 °C reference, a thermally buffered indoor case and a weather-driven outdoor case are compared. The battery is cycled between 20% and 80% state of charge at discharge rates from 0.1C to 0.6C. The model predicts only a small climate-related RTE difference: relative to the constant reference, the Bangkok outdoor case is approximately 0.16-0.28 percentage points higher. At 0.6C, modeled RTE changes from 93.94% to 94.17%, while maximum pack temperature rises from 39.06 °C to 49.95 °C. The results indicate that tropical thermal exposure affects modeled pack temperature and operating margin much more strongly than short-term battery-side RTE.

Key words: residential battery storage, round-trip efficiency, $LiFePO_4$, tropical climate, Bangkok, thermal performance

INTRODUCTION

Residential battery systems are increasingly combined with photovoltaic generation to increase self-consumption and shift locally generated electricity to later periods (Bagalini et al., 2019). Useful energy yield depends on battery-internal losses as well as converter, standby and auxiliary losses (Munzke et al., 2021).

Round-trip efficiency is therefore an important storage-performance indicator, but its interpretation depends on the selected measurement boundary. Battery-terminal DC efficiency excludes inverter and auxiliary losses included in wider system assessments (Conover et al., 2016; HTW Berlin Hochschule für Technik und Wirtschaft et al., 2019). The present work consequently uses a clearly defined battery-side DC boundary.

Temperature influences lithium-ion impedance, voltage response and degradation. Moderately higher temperature can reduce short-term resistance, whereas prolonged elevated temperature increases thermal stress and can accelerate ageing (Kucinskis et al., 2022; Liao et al., 2012; Ruiz et al., 2017). This distinction is particularly relevant in tropical installations, where batteries may operate in conditioned rooms, thermally buffered spaces or warmer outdoor environments. Studies under hot climates and Thai operating conditions likewise emphasize the importance of thermal exposure and temperature management (A'amar et al., 2025; Ketjoy et al., 2025).

Comparatively little attention has been given to short-term battery-side RTE of residential storage under representative tropical ambient conditions. This study therefore examines how Bangkok installation environments affect modeled DC-side RTE, pack temperature and operating margin while the battery configuration and cycling protocol are held constant.

[1] Corresponding author, matthias.hauer0404@gmail.com; ORCID: 0000-0000-0000-0000
[2] ashish.mexpert@gmail.com; ORCID: 0000-0000-0000-0000
[3] momir.tabakovic@technikum-wien.at; ORCID: 0000-0000-0000-0000

MATERIAL AND METHODS

Battery Model and System Boundary

A reduced-order electro-thermal battery model was implemented in Python. The nominal pack configuration is 48 V and 314 Ah. The parameter set represents a residential battery configuration for comparative simulation and is not presented as a manufacturer-specific digital twin.

The reported efficiency boundary is located at the battery DC terminals. Inverter conversion, AC-side losses, standby consumption, auxiliary loads and the energy demand of room conditioning are excluded.

A practical inverter-battery setup supported system familiarization and qualitative plausibility checks during the original study, but did not provide a controlled temperature-dependent RTE validation campaign. The numerical results are therefore interpreted as model-based comparisons.

***Table 1**. Main simulation parameters.*

Parameter	Value	Parameter	Value
Nominal voltage	48 V	Nominal capacity	314 Ah
SOC window	20-80%	Charge rate	0.30C
Discharge rates	0.1C-0.6C	Time step	5 min
Max. charge current	100 A	Max. discharge current	250 A
Reference resistance	0.012 Ω	Pack mass	130 kg
Effective c_p	950 J/(kg K)	hA	18 W/K
Model thermal cutoff	55 °C	Re-enable threshold	50 °C

The thermal parameters and reference resistance are engineering model assumptions rather than manufacturer-certified properties.

Electro-Thermal Model

Open-circuit voltage is represented as a piecewise function of SOC, consistent with the relatively flat mid-SOC behaviour of $LiFePO_4$ batteries (Roscher & Sauer, 2011; Weng et al., 2013; Zhu et al., 2015).

Internal resistance is modeled as

$$\boldsymbol{R_{\mathrm{int}} = 0.012\, F_T(T)\left[1 + 0.45(1 - \mathrm{SOC})^{1.5}\right].} \quad (1)$$

Where

$$\boldsymbol{F_T(T) = \begin{cases} \exp[0.03(25 - T)], & T < 25^{\circ}\mathrm{C}, \\ \exp[-0.01(T - 25)], & T \geq 25^{\circ}\mathrm{C}. \end{cases}} \quad (2)$$

The direction of this dependence is consistent with published temperature- and SOC-dependent $LiFePO_4$ behaviour (Liao et al., 2012; Safoutin et al., 2015). At unchanged SOC, the model resistance is approximately 9.5% lower at 35 °C and 13.9% lower at 40 °C than at 25 °C. At 50% SOC, for example, the corresponding modeled values are approximately 13.91, 12.59 and 11.97 mΩ.

Terminal voltage and DC power are calculated as

$$\boldsymbol{V_{\mathrm{term}} = V_{\mathrm{OCV}} - IR_{\mathrm{int}}, \qquad P_{\mathrm{DC}} = V_{\mathrm{term}} I.} \quad (3)$$

where positive current denotes discharge.

Pack temperature is represented by the lumped balance

$$mc_p \frac{\mathrm{d}T_{\mathrm{pack}}}{\mathrm{d}t} = I^2 R_{\mathrm{int}} - hA\left(T_{\mathrm{pack}} - T_{\mathrm{amb}}\right). \quad (4)$$

This reduced-order model does not resolve internal temperature gradients, enclosure radiation or detailed airflow (Forgez et al., 2010; Song et al., 2021). Equation (4) nevertheless captures the two effects central to this study: resistive heat generation and heat exchange with the ambient environment.

Weather Dataset and Ambient Scenarios

The outdoor scenario uses hourly air-temperature observations from Meteostat (Lamprecht, 2026). The reproducible comparison configuration uses Meteostat/WMO station 48455 (Bangkok, Thailand; approximately 13.7333° N, 100.5667° E; elevation 2 m), for which station metadata are provided by Meteostat (Meteostat, n.d.).

The weather interval is 1 March 2025 at 00:00 through 31 March 2025 at 23:00 local Bangkok time. Only hourly air temperature is used by the battery model. Missing temperature values, if present, are linearly interpolated in the hourly series. The hourly observations are subsequently expanded to the 5 min simulation grid by forward filling.

Three thermal environments are compared. The reference case uses a constant 25 °C. The outdoor case uses the Meteostat temperature series directly. The buffered indoor case is derived from the same outdoor series according to

$$T_{\mathrm{target},k} = 30 + 0.45\left(T_{\mathrm{out},k} - 30\right), \quad (5)$$

followed by

$$T_{\mathrm{in},k} = T_{\mathrm{in},k-1} + \frac{\Delta t}{12\ \mathrm{h}}\left(T_{\mathrm{target},k} - T_{\mathrm{in},k-1}\right). \quad (6)$$

The indoor case is an engineering representation of thermal buffering, not a complete building-energy model.

Cycling, Protection and RTE Averaging

Each C-rate case is simulated independently over the same monthly time window. Every run begins at the first timestamp of its ambient series with an initial SOC of 80% and an initial pack temperature equal to the corresponding ambient temperature.

The battery discharges toward 20% SOC and is subsequently charged toward 80%. Charging is requested at 0.30C, while discharge rates from 0.1C to 0.6C are evaluated. SOC is updated through Coulomb counting,

$$\mathrm{SOC}_{k+1} = \mathrm{SOC}_k - \frac{I_k \Delta t}{Q}. \quad (7)$$

A simplified supervisory layer imposes current, voltage and SOC limits. A pack temperature of 55 °C is used as a conservative model protection threshold rather than as a claimed manufacturer BMS setting. Published $LiFePO_4$ ageing research recommends substantially lower temperatures for normal operation and identifies 55 °C as an upper temperature that should not be exceeded (Xu et al., 2025). Operation is re-enabled below 50 °C, providing a 5 °C model hysteresis band. No thermal trip occurs in the reported cases.

For completed cycle j, DC-side RTE is

$$\eta_{\mathrm{RTE},j} = \frac{E_{\mathrm{dis},j}}{E_{\mathrm{ch},j}}. \quad (8)$$

The value reported as "average cycle RTE" is the arithmetic mean of all completed-cycle efficiencies within the monthly window,

$$\overline{\eta}_{\mathrm{RTE}} = \frac{1}{N}\sum_{j=1}^{N} \eta_{\mathrm{RTE},j}. \tag{9}$$

A cycle still incomplete at the end of the month is excluded. The numbers of completed cycles at 0.1C, 0.2C, 0.3C and 0.4C are 92, 146, 182 and 207, respectively, in all three scenarios. At 0.5C the reference, indoor and outdoor cases contain 270, 250 and 249 completed cycles; at 0.6C the corresponding counts are 318, 317 and 290.

SOC transitions are evaluated on the finite 5 min grid without sub-step interpolation. Differences of only a few tenths of a percentage point are therefore interpreted as comparative model trends rather than measurement-level accuracy.

RESULTS AND DISCUSSION

Table 2 summarizes modeled average cycle RTE and peak pack temperature. Increasing discharge rate decreases modeled RTE in all three environments. The climate-related separation between the three RTE series remains small.

***Table 2**. Modeled average cycle RTE and maximum pack temperature.*

C-rate	Ref. RTE [%]	Indoor RTE [%]	Outdoor RTE [%]	Ref. $T_{pack,max}$ [°C]	Indoor $T_{pack,max}$ [°C]	Outdoor $T_{pack,max}$ [°C]
0.1C	96.90	96.97	97.06	29.63	32.10	40.28
0.2C	96.20	96.28	96.39	30.40	32.86	40.94
0.3C	95.54	95.63	95.76	31.49	33.94	42.45
0.4C	94.93	95.02	95.17	34.46	36.88	45.25
0.5C	94.44	94.55	94.72	36.85	39.39	47.26
0.6C	93.94	94.06	94.17	39.06	41.79	49.95

Figure 1 shows that the effect of discharge rate is much larger than the separation between ambient scenarios.

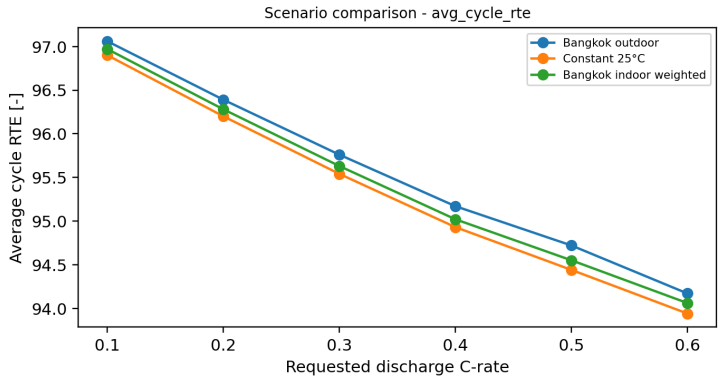


***Fig. 1**. Modeled average cycle DC-side RTE versus requested discharge C-rate.*

Within the implemented model, the Bangkok outdoor case produces an average cycle RTE approximately 0.16-0.28 percentage points above the constant-reference case. This direction follows from the modeled temperature dependence of internal resistance: higher pack temperature reduces R_{int} and therefore reduces resistive voltage loss. Because resistive loss represents only part of the battery-side energy balance, however, the resulting change in total modeled RTE remains small.

This modest electrical effect must be considered together with the substantially stronger thermal response. Across the investigated rates, peak pack temperature in the outdoor case is approximately 10 °C to 11 °C above the reference. At 0.6C, modeled RTE changes from 93.94% to 94.17%, whereas peak pack temperature increases from 39.06 °C to 49.95 °C. The latter remains below the model cutoff but leaves considerably less thermal margin.

These two observations result from the same electro-thermal model and are not contradictory. Equation (2) reduces modeled electrical resistance as temperature rises, while Eq. (4) shows that warmer ambient air simultaneously reduces the temperature difference available for heat rejection. Consequently, a warmer pack can exhibit slightly lower resistive losses while still reaching a markedly higher operating temperature.

The same resistance effect is also visible in the terminal-voltage response. At 0.3C, the minimum modeled terminal voltage is approximately 48.273 V in the reference case, 48.291 V indoors and 48.307 V outdoors. Although the warmer cases therefore show a small electrical benefit at this operating point, the magnitude of the voltage difference is minor compared with the accompanying change in thermal exposure.

Taken together, the results show why the predicted RTE increase should not be interpreted as evidence that hotter battery operation is preferable. Elevated temperature is associated with accelerated lithium-ion ageing (Ketjoy et al., 2025; Kucinskis et al., 2022; Ruiz et al., 2017). Within the scope of the present model, thermal buffering is therefore more relevant for preserving operating margin than for improving short-term battery-side RTE.

The numerical magnitude of the RTE separation remains model-dependent. The resistance relation, lumped thermal parameters, synthetic indoor temperature and finite time step introduce uncertainty, and the available practical setup did not provide controlled validation across the investigated climate cases. The sub-percentage-point differences should therefore be interpreted as trends predicted by the reduced-order model, not as experimentally established differences with two-decimal precision.

CONCLUSION

A reduced-order electro-thermal model was used to compare battery-side DC round-trip efficiency under a constant 25 °C reference and representative indoor and outdoor Bangkok conditions.

Increasing discharge rate from 0.1C to 0.6C reduces modeled RTE in all three scenarios. Within the implemented model, the Bangkok outdoor case produces an average RTE only 0.16-0.28 percentage points above the constant reference because modeled internal resistance decreases at higher pack temperature.

The thermal effect is considerably larger. At 0.6C, modeled RTE changes from 93.94% to 94.17%, while maximum pack temperature changes from 39.06 °C to 49.95 °C. The result therefore indicates greater sensitivity of thermal operating margin than of short-term battery-side RTE to tropical exposure.

Because the model has not been validated to sub-percentage-point accuracy, the small RTE difference is interpreted as a comparative model trend. For practical residential storage assessment, battery-side efficiency should be considered together with thermal exposure rather than used as an isolated indicator.

REFERENCES

A'amar, K., Sajid, M. U., Bicer, Y., & Al-Ansari, T. (2025). Thermal assessment of pole integrated LiFePO4 energy storage system for arid and non maintainable locations: A case study in Qatar. *Journal of Power Sources, 660*, 238444. https://doi.org/10.1016/j.jpowsour.2025.238444

Bagalini, V., Zhao, B. Y., Wang, R. Z., & Desideri, U. (2019). Solar PV-battery-electric grid-based energy system for residential applications: System configuration and viability. *Research, 2019*, 3838603. https://doi.org/10.34133/2019/3838603

Conover, D. R., Ferreira, S. R., Crawford, A. J., Schoenwald, D. A., Fuller, J., Rosewater, D. M., Gourisetti, S. N., & Viswanathan, V. (2016). *Protocol for uniformly measuring and expressing the performance of energy storage systems* (Tech. Rep. No. PNNL-22010 Rev. 2). Pacific Northwest National Laboratory.

Forgez, C., Do, D. V., Friedrich, G., Morcrette, M., & Delacourt, C. (2010). Thermal modeling of a cylindrical LiFePO4/graphite lithium-ion battery. *Journal of Power Sources, 195*(9), 2961-2968. https://doi.org/10.1016/j.jpowsour.2009.10.105

HTW Berlin Hochschule für Technik und Wirtschaft, BSW-Solar, & ZVEH. (2019, July). *Effizienzleitfaden für PV-Speichersysteme Version 2.0.1* (Tech. Rep.). HTW Berlin.

Ketjoy, N., Mensin, Y., Mensin, P., Kaewpanha, M., Khakhu, S., Chantarapongphan, C., & Sulaiman, S. I. (2025). Development of a degradation model for lifespan prediction: A case study on grid-scale battery energy storage systems in Thailand. *Batteries, 11*(11), 429. https://doi.org/10.3390/batteries11110429

Kucinskis, G., Bozorgchenani, M., Feinauer, M., Kasper, M., Wohlfahrt-Mehrens, M., & Waldmann, T. (2022). Arrhenius plots for Li-ion battery ageing as a function of temperature, C-rate, and ageing state - an experimental study. *Journal of Power Sources, 549*, 232129. https://doi.org/10.1016/j.jpowsour.2022.232129

Lamprecht, C. S. (2026). *Meteostat Python* [Official software documentation and citation metadata]. Meteostat.

Liao, L., Zuo, P., Ma, Y., Chen, X., An, Y., Gao, Y., & Yin, G. (2012). Effects of temperature on charge/discharge behaviors of LiFePO4 cathode for Li-ion batteries. *Electrochimica Acta, 60*, 269-273. https://doi.org/10.1016/j.electacta.2011.11.041

Meteostat. (n.d.). *Bangkok - weather station 48455* [Station metadata: 13.7333 N, 100.5667 E, elevation 2 m]. Meteostat. Retrieved September 22, 2026, from https://meteostat.net/en/station/48455

Munzke, N., Schwarz, B., Büchle, F., & Hiller, M. (2021). Evaluation of the efficiency and resulting electrical and economic losses of photovoltaic home storage systems. *Journal of Energy Storage, 33*, 101724. https://doi.org/10.1016/j.est.2020.101724

Roscher, M. A., & Sauer, D. U. (2011). Dynamic electric behavior and open-circuit-voltage modeling of LiFePO4-based lithium ion secondary batteries. *Journal of Power Sources, 196*(1), 331-336. https://doi.org/10.1016/j.jpowsour.2010.06.098

Ruiz, V., Kriston, A., Adanouj, I., Destro, M., Fontana, D., & Pfrang, A. (2017). Degradation studies on lithium iron phosphate-graphite cells. The effect of dissimilar charging-discharging temperatures. *Electrochimica Acta, 240*, 495-505. https://doi.org/10.1016/j.electacta.2017.03.126

Safoutin, M., Cherry, J., McDonald, J. F., & Lee, S. (2015). Effect of current and SOC on round-trip energy efficiency of a lithium-iron phosphate (LiFePO4) battery pack. *SAE 2015 World Congress and Exhibition*, 2015-01-1186. https://doi.org/10.4271/2015-01-1186

Song, S., Munk-Nielsen, S., Knap, V., & Uhrenfeldt, C. (2021). Performance evaluation of lithium-ion batteries (LiFePO4 cathode) from novel perspectives using a new figure of merit, temperature distribution analysis, and cell package analysis. *Journal of Energy Storage, 44*, 103413. https://doi.org/10.1016/j.est.2021.103413

Weng, C., Sun, J., & Peng, H. (2013). An open-circuit-voltage model of lithium-ion batteries for effective incremental capacity analysis. *Proceedings of the ASME 2013 Dynamic Systems and Control Conference*, V001T05A002. https://doi.org/10.1115/DSCC2013-3979

Xu, J., Li, H., Hua, S., & Wang, H. (2025). Experimental investigation of grid storage modes effect on aging of LiFePO4 battery modules. *Frontiers in Energy Research, 13*, 1528691. https://doi.org/10.3389/fenrg.2025.1528691

Zhu, L., Sun, Z., Dai, H., & Wei, X. (2015). A novel modeling methodology of open circuit voltage hysteresis for LiFePO4 batteries based on an adaptive discrete Preisach model. *Applied Energy, 155*, 91-109. https://doi.org/10.1016/j.apenergy.2015.05.103